Removal of *p*-Nitrophenol from Aqueous Solution Using Brazilian Peat: Kinetic and Thermodynamic Studies

S. Jaerger · A. dos Santos · A. N. Fernandes · C. A. P. Almeida

Abstract Removal of *p*-nitrophenol (PNP) from aqueous solutions using fibrous peat has been investigated in this study by batch adsorption experiments. Factors that can affect the adsorption process, such as pH, temperature, initial PNP concentration and contact time, have been investigated. Fourier transform infrared (FTIR) and thermogravimetric analysis (TGA) measurements have also been obtained in order to study the adsorption mechanism of PNP by peat. The Langmuir and Freundlich equations have been applied to investigate the equilibrium. The data fitted the Langmuir isotherm well, with the maximum adsorption capacity decreasing with temperature from 23.4 to 16.1 mg g^{-1}. In general, the adsorption equilibrium was attained within 100 min. For the kinetics study, the best fit was obtained by the pseudo-second-order model instead of the pseudo-first-order model, both of which applied to the experimental data, whereas the results of intraparticle diffusion show a two-step adsorption process. The activation energy value of 70.31 kJ mol^{-1}, calculated from the Arrhenius equation, indicated a predominantly chemical adsorption, whereas the thermodynamic parameters, obtained by the van't Hoff equation, were exothermic and spontaneous in nature.

S. Jaerger · A. dos Santos · C. A. P. Almeida
Departamento de Química, Universidade Estadual do Centro-Oeste, 85040-080 Guarapuava, PR, Brazil

A. N. Fernandes (✉)
Instituto de Química, Universidade Federal do Rio Grande do Sul, 91501-970 Porto Alegre, RS, Brazil
e-mail: andreia.fernandes@ufrgs.br

1 Introduction

In recent years, great attention has been given to nitroaromatic compounds in the environment. *p*-Nitrophenol (PNP) is a nitroaromatic compound that is widely used in many industries such as oil refineries, petrochemicals, coke ovens, pesticides and herbicides, among others. This compound, in bodies of water, affects water quality and can induce physical, chemical and biological changes in many species of animals and plants. Also, depending on the concentration level, water containing PNP can be toxic to both aquatic life and human health (Chang et al. 2009).

Owing to the increased discharge of organic contaminants in wastewater, it is very important to treat effluents containing such compounds before they reach the water bodies (Tang et al. 2007). In order to meet environmental regulations, several wastewater treatment technologies are available, among which advance oxidative processes (Oller et al. 2011), extraction processes and biodegradation (Yuan et al. 2012) stand out. However, in some cases, these processes are not satisfactory because of their high cost and that they can also generate secondary contaminants. The PNP molecule has a nitro group in its aromatic ring, which gives it resistance to chemical oxidation. Furthermore, anaerobic and biological degradation can generate hydroxyl and nitro compounds, which can be carcinogenic (Li

et al. 2009). Considering these aspects, the purification of wastewater contaminated with PNP is a great challenge for scientists and environmental engineers, and new technologies must be developed for the removal of PNP from industrial effluents.

Adsorption is widely used to remove contaminants from wastewater, owing to its performance, ease of operation and relatively simple regeneration. Adsorbent materials such as activated carbon (Huang et al. 2008; Shao et al. 2013; Ding et al. 2014), resins (Pan et al. 2006), montmorillonite (Almeida et al. 2009; Ye and Lemley 2009; Xue et al. 2013; Marco-Brown et al. 2014), organoclay (Ko et al. 2007), chitosan (Ngah and Fatinathan 2006), mineral waste from coal mining (Almeida et al. 2010), nanoparticles (Jing et al. 2013), cotton fibres (Liu et al. 2014a, b), magnetic adsorbents (Ma et al. 2014), montmorillonite clay modified with iron (Cottet et al. 2014), among others, have been used in order to remove PNP and other contaminants from aqueous solutions. In contrast, peat is an alternate, low-cost biosorbent of high porosity that does not require activation and is feasible in many tropical countries, including Brazil (Fernandes et al. 2007, 2011; Rovani et al. 2014).

Peat has many applications in remediation and soil conditioning as well as nutrient storage, as it is a material with high organic matter content. Using knowledge of the characteristics and composition of peat, it has become widely used and studied as an alternate material for the treatment of waters and effluents (Couillard 1994; Brown et al. 2000; Zhi-rong et al. 2008) in an adsorption processes (Twardowska et al. 1999; Petroni et al. 2000; Ringqvist et al. 2002; Fernandes et al. 2007, 2010a, 2011; Zhi-rong et al. 2008; Rovani et al. 2014). Several studies have been developed with peat, owing to its high capacity to remove contaminants such as metals, dyes, organic molecules and odours from domestic and industrial effluents (Couillard 1994). Researchers have suggested possible interactions between contaminants and peat through ion-exchange reactions, owing to the presence of polar functional groups such as alcohols, aldehydes, carboxylic acids, ketones and phenolic hydroxides, which may bond with the adsorbed pollutant species (Couillard 1994; Brown et al. 2000).

In this study, peat was used as the biosorbent in the removal of PNP from aqueous solutions. The effects of parameters such as initial concentration of PNP, contact time and temperature on the adsorption process were investigated. Kinetics, equilibrium and thermodynamic studies were also addressed.

2 Experimental

2.1 Chemicals

p-Nitrophenol (PNP) (molecular weight: 139.11 g mol^{-1}; molecular formula: $C_6H_5NO_3$; maximum wavelength: $\lambda_{max}=400$ nm) was supplied by Vetec and used without further purification. A PNP stock solution was prepared by dissolving an accurately weighed quantity of PNP in deionised water in volumetric flasks to achieve a concentration of 2000 mg L^{-1}. Working PNP solutions were obtained by diluting the PNP stock solution to the required concentration (50–1500 mg L^{-1}). All reagents used in this study were of adequate purity for the analyses (analytical grade).

2.2 Biosorbent Preparation and Characterization

The peat sample used in this study was collected in a peat land in the Arroio do Silva Beach (Santa Catarina State, South of Brazil). It was classified as fibrous peat (FP) according to the International Peat Society (IPS) (Fernandes et al. 2007; Girardello et al. 2013). The peat was air dried and sieved to give a 50–150 mm size fraction using ASTM standard sieves; it was then acidified in a separation funnel using 1.0 mol L^{-1} HCl (10 mL). Then, it was rinsed with deionised water until the pH reached a value 5 and dried at 60 °C for a period of 24 h. Typical characteristics of the peat (such as acidity, density and ash content) have already been obtained in previously studies (Fernandes et al. 2007, 2010b).

The biosorbent (FP) was characterised by vibrational spectroscopy in the infrared region with Fourier transform (FTIR) using a Shimadzu Prestige-21 spectrometer (California, USA). The spectrum was obtained with a resolution of 4 cm^{-1} with 64 cumulative scans. Pellets were prepared by pressing a mixture of 1 mg of peat and 100 mg of KBr (spectroscopy grade) under vacuum. Thermogravimetric analysis (TGA) was performed using a Seiko Instrumentation Inc. thermogravimetric/ differential thermal analyser (TG/DTA 6300; Tokyo, Japan). The sample (ca. 10 mg) was placed in a platinum crucible and heated from 30 to 1000 °C under an atmosphere of nitrogen (50 mL min^{-1}) at a heating rate of 10 °C min^{-1}. Additional characterisation has been presented in a previous study (Fernandes et al. 2010b; Girardello et al. 2013).

2.3 Adsorption Method

Batch uptake studies were conducted by placing 100 mg of peat in contact with 50 mL of PNP solution of varying initial concentrations from 50 to 1000 mg L^{-1} at pH 8. The pH study was performed by comparing the solutions containing PNP (600 mg L^{-1}) with acidic and basic pH values for a period of 240 min. The flasks with their contents were then shaken throughout the experiments at different adsorption temperatures of 15, 25 and 35 °C. The stirring speed was kept constant at 500 rpm. Blanks were used to correct the absorbance for the presence of dissolved organic matter. At the end of each adsorption period, a 100 μL aliquot was collected, diluted, homogenised and centrifuged (Centribio 80-2B; São Paulo, Brazil) for 10 min at 2000 rpm. The concentration of PNP in the supernatant solution, before and after adsorption, was determined spectrophotometrically using a calibration curve in a Varian Cary 50 UV/Vis (California, USA) diode array spectrophotometer with a 1 cm path length cell at $\lambda_{max}=400$ nm.

The amount of PNP adsorbed at each time interval and the percentage removal of PNP (%) by the peat were calculated by applying Eqs. (1) and (2), respectively:

$$q = \frac{(C_0 - C_f)}{m} \cdot V \quad (1)$$

$$\%Removal = 100 \cdot \frac{(C_0 - C_f)}{C_0} \quad (2)$$

where q is the amount of PNP adsorbed by the adsorbent (mg g^{-1}), C_0 is the initial PNP concentration in contact with the adsorbent (mg L^{-1}), C_f is the PNP concentration (mg L^{-1}) after the batch adsorption process, m (g) is the mass of adsorbent and V is the volume of PNP solution (L).

3 Results and Discussion

3.1 Biosorbent Properties

Figure 1a, b shows the FTIR spectra of the FP before and after adsorption of PNP, respectively. In general, the spectra present similar characteristics, with typical absorption bands of natural organic matter (Fernandes et al. 2010b; Girardello et al. 2013). The major infrared absorptions observed included two peaks at 2923 and
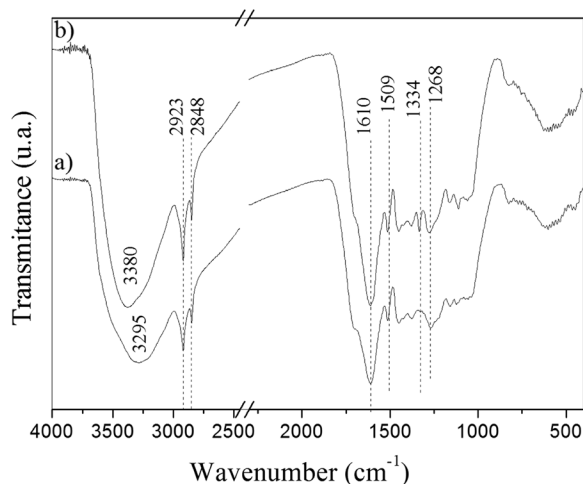

Fig. 1 FTIR vibrational spectra for the peat (**a**) and peat + PNP (**b**). The number indicated for each band corresponds to a wavenumber expressed in cm^{-1}

2848 cm^{-1}, corresponding to asymmetric and symmetric C–H stretching of the CH_2 groups of aliphatic hydrocarbons, respectively; a band at 1610 cm^{-1} assigned to C=C stretching, C=O stretching of COO–, ketonic C=O and aromatic C=C conjugated with COO–; a peak at 1509 cm^{-1} attributed to N–H deformation, C–N stretching vibration and C=C aromatic bounds; a peak at 1268 cm^{-1}, corresponding to aromatic C and C–O stretching and the region between 1250 and 1000 cm^{-1} attributed to C–O stretching of aryl esters, esters and phenols (Antunes et al. 2012; Girardello et al. 2013). The main differences observed in the FTIR spectra were related to the bands at 3300 and 1330 cm^{-1}. The absorption band at 3300 cm^{-1}, assigned to O–H stretching, was shifted after adsorption (Fig. 1b), demonstrating an interaction between the peat surface and the phenolic group of the PNP. In addition, the peak at 1334 cm^{-1}, attributed to C–O–H stretching of bonds in carboxylic acids, was only present in the peat + PNP spectrum, demonstrating the effective adsorption of PNP in the biosorbent.

The thermogravimetric (TG) and derivative thermogravimetric (DTG) curves are shown in Fig. 2. In general, the thermal decomposition proceeds through three main stages. The first stage occurs in the temperature range of 62–65 °C and corresponds to the evaporation of water incorporated into or adsorbed onto the peat, which is accompanied by a slight weight loss (around 11 %). In the second and third stages, at temperatures of approximately 300 and 450 °C, weight losses of 29.8 and 38.6 % are observed for peat and 29.8 and 21.4 % for
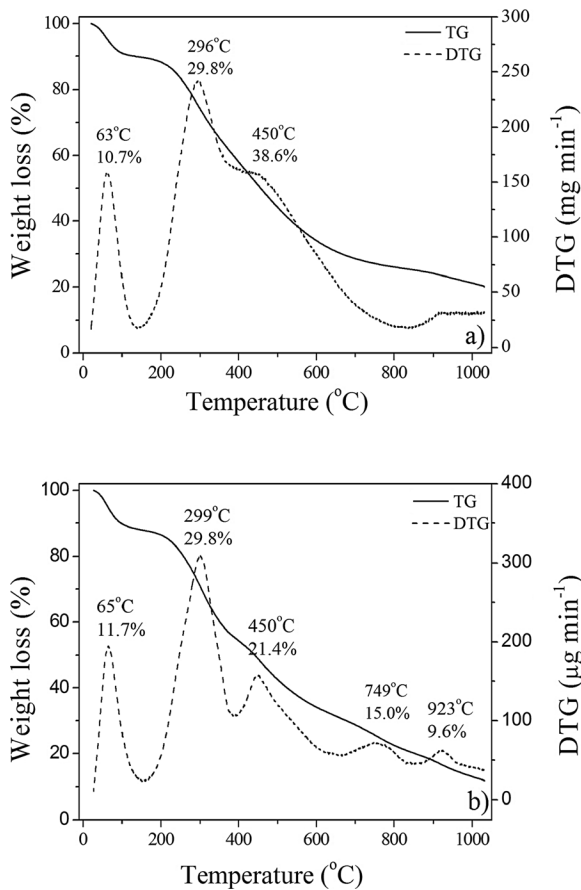
Fig. 2 TG (*solid line*) and DTG (*dash line*) curves of peat (**a**) and peat + PNP (**b**)

peat + PNP, respectively. This temperature range is related to the decomposition of organic compounds present in the peat sample (Fernandes et al. 2010b; Girardello et al. 2013). Two weight losses can be observed in the TG curve of peat + PNP (Fig. 2b), with the first peak at 749 °C with 15.0 % loss and the other at 923 °C with 9.6 % loss. Weight losses observed for temperatures higher than 600 °C are associated with phenomena such as reactions of silica and alumina at these temperatures as well as the development of new crystalline phases containing silicates (Goulart 1995).

3.2 Adsorption Parameters

The effects of initial pH on percentage of removal of PNP solution (600 mg L^{-1}) using fibrous peat were evaluated within the pH range 1–11. There is an acid–base balance in PNP solution, which presents in its acidic form at a wavelength ~315.0 nm, whereas the alkaline form has a

wavelength ~400.0 nm. According to the observed absorbance values, the adsorption of PNP into peat is not significant at acidic pH values (1–6) (10.20–25.52 %), because an ion–dipole interaction occurs between the peat and PNP, whereas hydrogen bonds occur between the hydroxyl group of PNP and the carboxyl groups present in the peat (Nourmohammadian et al. 2007). At pH values of 8–9, there was increased removal of PNP (40.58–56.76 %), which may be attributed to the exchange of electrons between peat and *p*-nitrophenolate ions (Erdem et al. 2009). At pH values of 10–11, the results were not affected by the presence of peat, because the *p*-nitrophenolate ions were not densely embedded in the surface of the peat, causing an electrostatic repulsion (Chang et al. 2009). On these aspects, pH 8 was chosen for the adsorption experiments.

The effects of the initial concentration and the removal percentage on PNP adsorption into peat at 25 °C are shown in Fig. 3. The results demonstrate that the percentage removal of PNP decreases with increasing PNP concentration at all temperatures studied. On the other hand, more PNP was retained by the peat when the initial PNP concentration increased, reaching a maximum at 1200 mg L^{-1}. Above this concentration, the adsorption equilibrium was established and the PNP concentration in the bulk solutions becomes a dynamic balance with that on the surface. This study provides information on the adsorption capacity of peat. In a fixed mass of adsorbent, increasing the amount of adsorbate causes the occupation of the adsorption sites to reach saturation in the surface layer. After saturation, no
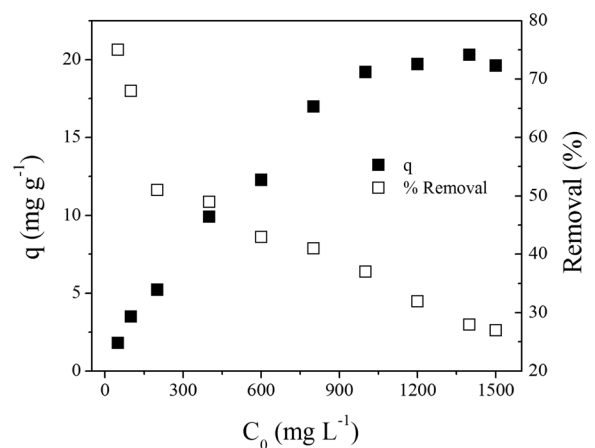

Fig. 3 Effects of the amount of PNP adsorbed (*q*) (**a**) and the initial PNP concentration (C_0) (**b**) on adsorption at 25 °C. Conditions: pH 8.0 and FP biosorbent mass 100.0 mg

more sites are available in the adsorbent and the adsorption capacity is attained.

In general, the amount of PNP adsorbed onto the peat increases with time, until it reaches the adsorption equilibrium (Fig. 4). As can be seen, there was rapid PNP removal during the first 20 min for all concentrations evaluated, owing to reduced binding sites in the peat (Saha et al. 2010). The saturation was established within approximately 50 min for concentrations of 50–1000 mg L^{-1} and within about 100 min for the other concentrations. This occurs because of the increased number of PNP molecules in solution, which can compete with each other through the pores of the biosorbent, contributing to the increased length of time required to reach the adsorption equilibrium (Liu et al. 2014a, b; Ma et al. 2014). The temperature variation caused a decrease in the adsorption capacity, mainly from 25 to 35 °C. The same trend was found in a study by Erdem et al. (2009), in which the decay of adsorption capacity was triggered because of the exothermic nature of the process.

3.3 Kinetic Studies

The study of adsorption kinetics is an important tool to better understand the rate at which contaminants are removed from aqueous solutions onto the surface of an adsorbent, which, in turn, controls the residence time of the adsorbate uptake at the solid–solution interface (Altenor et al. 2009). The pseudo-first-order and pseudo-second-order kinetic models were applied to
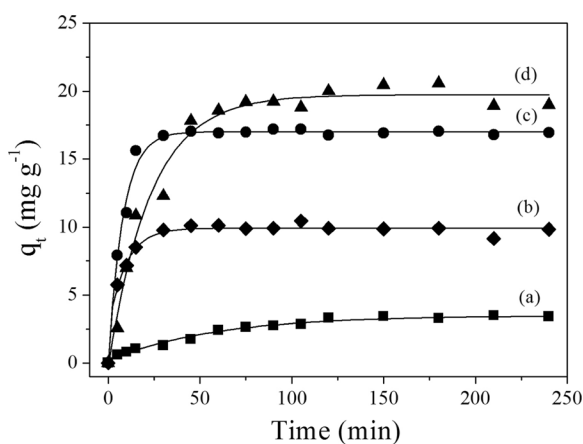

Fig. 4 Progressive removal of PNP from aqueous solutions using peat at concentrations of 100 (**a**), 400 (**b**), 800 (**c**) and 1500 mg L^{-1} (**d**) at 25 °C. Conditions: pH 8.0 and FP biosorbent mass of 100.0 mg

describe the adsorption processes in this study. The pseudo-first-order linear equation (Ho 2004) is given as

$$\ln(q_e - q_t) = \ln q_{e1} - k_1 t \qquad (3)$$

where q_{e1} (mg g^{-1}) represents the amount of PNP adsorbed at equilibrium, as calculated by the pseudo-first-order equation, k_1 (min^{-1}) is the adsorption rate constant for the pseudo-first-order reaction and t (min) is the time interval (Chang et al. 2009; Erdem et al. 2009; Li et al. 2009; Iram et al. 2010). According to Eq. (3), the plot of $\ln(q_e - q_t)$ versus t should give a straight line to be applicable with a high correlation coefficient. From the straight line, the values of k_1 and q_{e1} can be determined.

The pseudo-second-order linear equation can be given as

$$\frac{t}{q_t} = \frac{1}{k_2 q_{e2}^2} + \frac{t}{q_{e2}} \qquad (4)$$

where q_{e2} (mg g^{-1}) is the amount of PNP adsorbed at equilibrium, as calculated by the pseudo-second-order equation, and k_2 (g mg^{-1} min^{-1}) is the adsorption rate constant for the pseudo-second-order reaction (Chang et al. 2009; Erdem et al. 2009). The constants k_2 and q_{e2} can be calculated from the straight line plot of t/q_t versus t.

The values of the kinetic parameters for PNP removal using peat are shown in Table 1. As can be seen, the adsorption data fit better to the pseudo-second-order kinetic model than the pseudo-first-order model. The linear correlation coefficients of the pseudo-second-order reaction are above 0.99 for all initial PNP concentrations and for the three temperatures studied (Fig. 5). Furthermore, the experimental q_e ($q_{e,exp}$) data are closer to the values obtained using the pseudo-second-order kinetic model, indicating that the overall process is both dependent on the amount of PNP and on the available sites in the peat (Fernandes et al. 2007; Chang et al. 2009; Erdem et al. 2009; Li et al. 2009; Almeida et al. 2010).

The effect of intraparticle diffusion resistance on adsorption can be evaluated using a model based on the theory proposed by Weber and Morris (1963), as described by Eq. 5:

$$q_t = k_i t^{0.5} + C \qquad (5)$$

where k_i is the rate constant (mg g^{-1} t$^{-0.5}$) and values of C give information regarding the thickness of the boundary layer (Hu et al. 2010). A plot of q_t against

Table 1 Kinetic parameters and intraparticle diffusion for PNP removal using a peat adsorbent

T (°C)	C_0 (mg L^{-1})	$q_{e,exp}$ (mg g^{-1})	Pseudo-first-order			Pseudo-second-order			Intraparticle diffusion		
			$10^{-2}k_1$ (min^{-1})	q_{e1} (mg g^{-1})	R_1	$10^{-2}k_2$ (g mg^{-1} min^{-1})	q_{e2} (mg g^{-1})	R_2	$10^{-2} k_i$ (mg g^{-1} h$^{-0.5}$)	C	R_i
15	50	2.05	14.94	1.21	0.9730	34.1	2.12	0.9999	4.56	1.22	0.9729
	100	3.00	2.86	1.00	0.9156	12.8	3.12	0.9995	11.70	0.81	0.9832
	200	5.49	5.18	2.83	0.9766	5.63	5.95	0.9935	23.73	2.25	0.9967
	400	10.37	1.36	4.62	0.9299	1.16	10.39	0.9984	40.12	3.80	0.9801
	600	13.76	1.51	3.93	0.7383	1.18	14.40	0.9968	162.48	2.38	0.9831
	800	17.51	2.34	5.05	0.7390	0.92	17.95	0.9991	148.29	4.81	0.9968
	1000	20.49	2.85	13.05	0.8408	0.29	22.03	0.9958	174.30	1.10	0.9922
	1200	20.81	3.16	13.27	0.9440	0.45	21.99	0.9979	206.24	2.12	0.9840
	1400	21.38	0.78	6.47	0.6929	0.59	27.65	0.9959	201.16	8.23	0.9756
	1500	21.14	1.24	5.61	0.7759	1.28	20.90	0.9993	114.46	8.48	0.9955
25	50	1.82	1.92	1.12	0.9370	3.32	2.00	0.9916	8.80	0.24	0.9826
	100	3.51	2.02	3.53	0.9192	3.87	3.51	0.9944	12.61[b]	0.82	0.9825
	200	5.23	2.08	1.54	0.9176	3.23	7.07	0.9993	15.39	2.44	0.9928
	400	9.91	1.31	1.41	0.5734	3.37	10.49	0.9988	39.42	4.41	0.9681
	600	12.27	1.37	1.95	0.4873	3.21	12.99	0.9997	48.55	5.70	0.9972
	800	17.00	1.70	1.67	0.5956	3.49	17.11	0.9997	248.66	0.50	0.9945
	1000	19.20	2.86	6.08	0.8049	1.87	19.49	0.9994	150.98	5.75	0.9780
	1200	19.71	2.27	19.45	0.9405	1.04	19.99	0.9964	198.11	0.08	0.9977
	1400	20.30	2.11	7.43	0.7269	1.34	20.43	0.9986	228.24	0.13	0.9996
	1500	19.63	1.40	6.66	0.7231	1.09	19.96	0.9956	236.54	1.85	0.9504
35	50	2.40	5.73	0.12	0.8097	232.80	2.41	0.9999	1.18	1.56	0.9916
	100	3.90	21.07	2.93	0.9913	19.36	4.06	0.9998	54.39	0.03	0.9947
	200	6.50	3.62	5.03	0.9612	1.16	7.35	0.9982	60.73	1.36	0.9973
	400	8.60	1.23	4.75	0.9667	0.94	8.58	0.9977	56.80	2.41	0.9990
	600	11.14	1.16	5.04	0.8988	1.03	11.41	0.9983	67.94	4.51	0.9921
	800	11.80	1.53	3.42	0.9782	1.66	11.94	0.9994	43.13	7.35	0.9960
	1000	12.70	1.07	3.86	0.8539	1.91	12.34	0.9996	136.54	4.99	0.9978
	1200	13.60	7.14	8.96	0.9418	1.18	17.29	0.9937	148.50	6.29	0.9746
	1400	14.20	0.47	14.05	0.9243	4.35	15.20	0.9917	308.94	0.18	0.9946
	1500	13.50	0.71	2.38	0.4349	5.57	12.90	0.9963	374.28	0.22	0.9896

Conditions: pH 8.0 and mass of adsorbent 100.0 mg

$t^{0.5}$ should give a linear graph, where the slope is k_i if the adsorption mechanism follows the intraparticle diffusion process. However, the data of this study (Fig. 6) exhibit multi-linear plots; therefore, the process is governed by two steps. This reveals that more than one mode of adsorption takes place in the uptake of PNP by peat. The initial linear portion might be attributed to the immediate adsorbing sites available on peat surface, and the later linear portion refers to gradual adsorption at the final equilibrium stages, in which intraparticle diffusion starts to slow down and level out because of the low PNP concentration remaining in the solution or because maximum adsorption is attained (Hu et al. 2010; Bhatnagar et al. 2010). The slope of the second linear portion of the plots has been defined as a rate parameter (k_i), which characterises the rate of adsorption when pore diffusion is rate limiting, according to Table 1. These results suggest that the adsorption of PNP onto peat is controlled by external mass transfer followed by intraparticle diffusion mass transfer
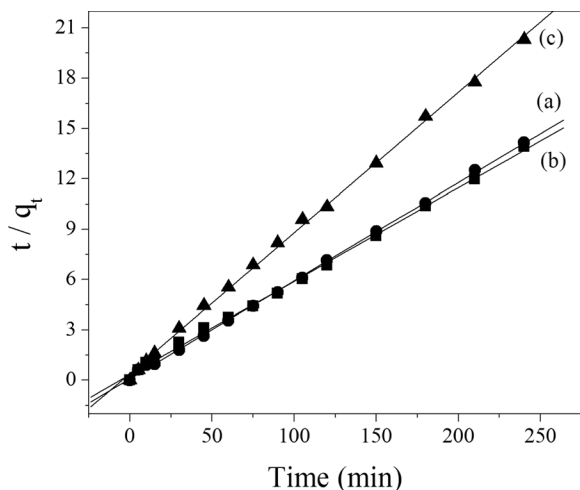
Fig. 5 Pseudo-second-order kinetics of PNP adsorption onto peat at 25 (**a**), 35 (**b**) and 45 °C (**c**). Conditions: pH 8.0, FP biosorbent mass of 100.0 mg and C_0=800 mg L^{-1}

(Arasteh et al. 2010). The values of C can determine the boundary thickness, as larger C values correspond to greater boundary layer diffusion effects (Yao et al. 2010, 2014. According to Table 1, C and k_i values decreased with increasing temperature (15–25 °C) in the concentration range of 600–1200 mg L^{-1}.

The activation energy of the adsorption process is found through the plot of $\ln k'_2$ versus $1/T$, according to the Arrhenius equation, given as

$$\ln k'_2 = \ln A - \frac{E_a}{RT} \tag{6}$$

where k'_2 is the pseudo-second-order rate constant for adsorption (g mol^{-1} s^{-1}), E_a is the activation energy
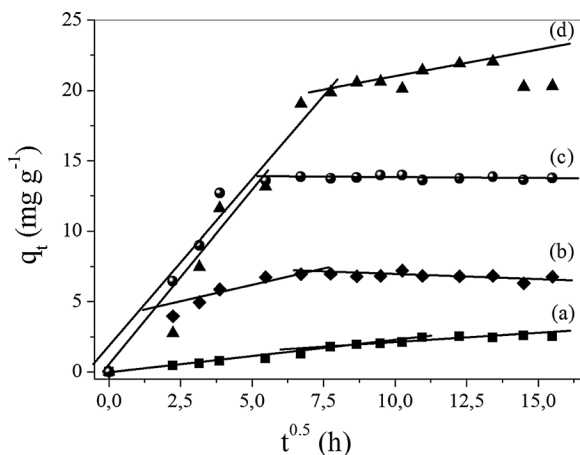

Fig. 6 Intraparticle diffusion model for PNP adsorption onto peat at 25 °C for concentrations of 100 (**a**), 400 (**b**), 800 (**c**) and 1000 mg L^{-1} (**d**)

(J mol^{-1}), A is the temperature-independent pre-exponential factor, R is the gas constant (8.314 J K^{-1} mol^{-1}) and T is the solution temperature (K). On the basis of a plot of $\ln k'_2$ versus $1/T$, E_a can be estimated from the slope of what should be a straight line passing through the points. The value of E_a may indicate whether the adsorption process is physical or chemical. For physisorption, the value lies in the range of 50–40 kJ mol^{-1}, whereas for the chemisorption, the value is in the 40–800 kJ mol^{-1} range (Erdem et al. 2009). The E_a was found to be 70.31 kJ mol^{-1}, which is a high potential barrier for the adsorption process and, therefore, corresponds to chemisorption.

3.4 Equilibrium Studies

Adsorption isotherms can show how molecules are distributed between liquid and solid phases when the adsorption process reaches an equilibrium state, indicating the interaction level between an adsorbate and an adsorbent. The adsorption of an adsorbate from one phase to the surface of another in a specific system leads to a thermodynamically defined distribution of the adsorbate between the phases as the system reaches equilibrium (Khenifi et al. 2009). Thus, the correlation of data by theoretical or empirical equations is essential for the practical design of adsorption systems (Chang et al. 2009). In this study, data were adjusted according to the Langmuir and Freundlich models. The Langmuir model is generally used with the assumption of ideal surface adsorption that is entirely homogeneous, whereas the Freundlich model is suitable for a heterogeneous system (Freundlich 1906; Li et al. 2009). The linear form of the Langmuir isotherm (Langmuir 1916; Fernandes et al. 2007) is usually given as

$$\frac{C_e}{q_e} = \frac{1}{q_{max} K_L} + \frac{C_e}{q_{max}} \tag{7}$$

where q_e (mg g^{-1}) is the amount of PNP adsorbed per unit mass of peat at equilibrium and K_L (L mg^{-1}) is the Langmuir constant related to the affinity of the binding sites; q_{max} (mg g^{-1}) is a parameter related to the maximum amount of PNP per unit weight of peat, which is defined as the monolayer saturation capacity, representing the maximum adsorption capacity of the adsorbent for a particular adsorbate (Li et al. 2009). K_L and q_{max} are Langmuir constants found from the

Table 2 Parameters of Langmuir isotherms and Freundlich for adsorption of PNP onto peat

T (°C)	Langmuir			Freundlich		
	K_L (L mg^{-1})	q_{max} (mg g^{-1})	r_L	K_F (L g^{-1})	n	r_F
15	0.0095	23.39	0.9978	0.5313	1.85	0.9858
25	0.0068	22.90	0.9980	0.4962	1.82	0.9661
35	0.0053	16.10	0.9955	2.1813	3.77	0.9847

Conditions: pH 8.0 and mass of adsorbent 100.0 mg

intercept and slope of the straight line of the plot C_e/q_e versus C_e, respectively.

The Freundlich isotherm is an empirical equation and is satisfactory for low concentrations of adsorbate (Li et al. 2009). The linear form of the Freundlich isotherm (Freundlich 1906) is given as

$$\ln q_e = \ln K_F + \frac{1}{n} \ln C_e \qquad (8)$$

where K_F (mg L^{-1}) is the Freundlich constant and n is a parameter related to the intensity of adsorption and to the system heterogeneity. K_F and n are Freundlich constants found from the intercept and slope of the straight line of the plot ln q_e versus ln C_e, respectively.

The parameter related to the maximum amount of PNP per unit weight of peat (q_{max}) indicates the theoretical monolayer saturation capacity. The q_{max} values decreased from 23.39 to 16.10 mg g^{-1} as a function of temperature (Table 2). Moreover, these q_{max} values are quite significant for PNP removal when compared to surfactant-modified clinoptilolite–polypropylene hollow fibre composites, nano-titanium dioxide and bismuth ferrocyanide, as can be seen in Table 3 (Nouri and Hagheseresht 2004; Krasil'nikova et al. 2008; Mehrizad et al. 2012; Motsa et al. 2012; Yao et al. 2014; Ofomaja and Unuabonah 2013; Tewari 2014). The values of K_L and K_F, as well as their correlation coefficients, r_F and r_L, are shown in Table 2. Based on the correlation coefficients, the fit of the Langmuir

Table 3 Adsorption capacities of nitrophenol compounds on various adsorbents

Adsorbents	Removed compounds	Adsorption capacity q_{max} (mg g^{-1})	Temperature (°C)	C_0 (mg L^{-1})	pH	References
Brazilian peat	p-Nitrophenol	23.39	15	50 to 1500	8	Present study
Surfactant-modified clinoptilolite–polypropylene hollow fibre composites	2.4.6-Trichlorophenol Ortho-nitrophenol	19.40 1.51	28	3 to 150	4 to 6 2 to 6	Motsa et al. 2012
ox-SWNTs	p-Nitrophenol	206.13	20	-	-	Yao et al. 2014
Activated charcoal	4-Nitrophenol	388.12	20	-	-	Krasil'nikova et al. 2008
Nano-titanium dioxide	4-Chloro-2-nitrophenol	17.53	25	2 to 10	2	Mehrizad et al. 2012
Mansonia sawdust	4-Nitrophenol	425.68	26	100	4	Ofomaja and Unuabonah 2013
Untrated activated carbon Trated activated carbon	p-Nitrophenol	222.58 225.36	28	-	2	Nouri and Hagheseresht 2004
BiFC	p-Aminophenol p-Nitrophenol	28.57 36.36	27	13.9 to 139	7	Tewari 2014
PbFC	p-Aminophenol p-Nitrophenol	44.44 50.00				
MnFC	p-Aminophenol p-Nitrophenol	66.67 80.00				

model to the experimental was better ($r_L > 0.99$) than the Freundlich model ($r_F < 0.98$), indicating the formation of a monolayer of PNP molecules on the peat surface (Li et al. 2009). Similar behaviour was observed by Ahmaruzzaman and Gayatri (2010) for the adsorption of PNP onto acid-activated jute stick char. Thus, PNP adsorption onto peat is limited to monolayer coverage with no significant interactions among neighbouring adsorbed molecules. It also means that the surface is relatively homogenous in terms of functional groups (Fernandes et al. 2010b) (Fig. 7).

3.5 Thermodynamic of Adsorption

Thermodynamic parameters, such as the Gibbs free-energy change, ($\Delta G°_{ads}$), enthalpy change ($\Delta H°_{ads}$) and entropy change ($\Delta S°_{ads}$), of an adsorption process are important in order to understand the kind of energy involved when molecules go to an adsorbent surface and how much of this energy is involved in the process. For PNP adsorption onto peat, $\Delta H°_{ads}$ and $\Delta S°_{ads}$ were determined from the van't Hoff equation (Iram et al. 2010):

$$\ln K'_L = \frac{\Delta S°_{ads}}{R} - \frac{\Delta H°_{ads}}{RT} \qquad (9)$$

where K'_L (L mol^{-1}) is the Langmuir equilibrium constant. The values of $\Delta H°_{ads}$ and $\Delta S°_{ads}$ were determined from the slope and intercept of the plot of ln K'_L versus $1/T$, respectively. $\Delta G°_{ads}$ values were calculated from Eq. 10 (Iram et al. 2010), as follows.
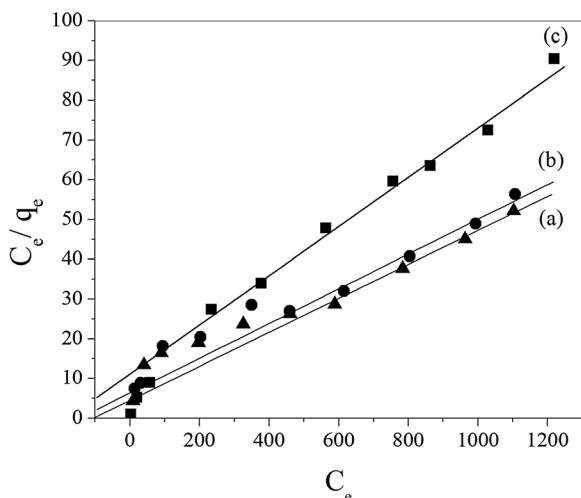
Fig. 7 Linear form of the Langmuir adsorption isotherm for the adsorption of PNP onto peat at 15 (**a**), 25 (**b**) and 35 °C (**c**). Conditions: pH 8.0 and FP biosorbent mass of 100.0 mg

Table 4 Thermodynamic parameters for the adsorption of PNP onto peat

T (°C)	$\Delta S°_{ads}$ (J K^{-1} mol^{-1})	$\Delta H°_{ads}$ (kJ mol^{-1})	$\Delta G°_{ads}$ (kJ mol^{-1})
15	−13.870	−21.171	−17.18
25			−17.04
35			−16.90

Conditions: pH 8.0 and mass of adsorbent 100.0 mg

$$\Delta G°_{ads} = -RT \ln K'_L \qquad (10)$$

The thermodynamic parameters of PNP adsorption onto peat are shown in Table 4. The negative values of $\Delta G°_{ads}$ at all temperatures confirmed the spontaneous nature of the adsorption process and the feasibility of the adsorption of PNP onto peat (Fernandes et al. 2010a). As can be seen, the increase in $\Delta G°_{ads}$ value with increasing temperature suggests a reduction in the spontaneous nature of the adsorption process, as the value of the modulus of decreases (Chowdhury et al. 2011). Adsorption with $\Delta G°_{ads}$ values between −20 and 0 kJ mol^{-1} correspond to physical processes, whereas those with values ranging from −400 to −80 kJ mol^{-1} correspond to chemisorption. A negative $\Delta G°_{ads}$ value for the adsorption process confirms that the adsorption of PNP onto peat is spontaneous (Iram et al. 2010). A negative $\Delta H°_{ads}$ value indicates an exothermic adsorption, whereas a negative $\Delta S°_{ads}$ ($\Delta S°_{ads} = -13.870$ kJ mol^{-1}) corresponds to a decrease in the degrees of freedom of the adsorbed species (Girardello et al. 2013). The negative $\Delta S°_{ads}$ value is corroborated by the decrease in the degrees the freedom of PNP, as the adsorption is not compensated by the increase of freedom of water from the peat surface (Romero-Gonzalez et al. 2005; Ozcan et al. 2006).

4 Conclusion

Peat was investigated to evaluate its performance in terms of the removal capacity of PNP from aqueous solutions. FTIR and TGA data of the peat sample studied showed typical characteristics of organic matter. In addition, the FTIR spectra before and after adsorption presented small differences, indicating the effective adsorption of PNP onto peat. The q_{max} values obtained by application of the Langmuir equation were 23.39, 22.90 and 16.10 mg g^{-1} at 15, 25 and 35 °C, respectively,

indicating an endothermic adsorption process. Based on the correlation coefficients of the kinetic models, the pseudo-second-order model was deemed more appropriate to describe the adsorption process, indicating that the overall process was dependent on the amount of PNP and the available sites in the peat. Intraparticle diffusion results show two steps, and k_i values obtained for the second step suggest that the adsorption of PNP onto peat is controlled by external mass transfer followed by intraparticle diffusion mass transfer. The E_a value and thermodynamic parameters showed that the nature of the adsorption process was exothermic and spontaneous. These aspects demonstrate the efficiency of adsorption of PNP onto peat.

References

Ahmaruzzaman, M., & Gayatri, S. L. (2010). Batch adsorption of 4-nitrophenol by acid activated jute stick char: equilibrium, kinetic and thermodynamic studies. *Chemical Engineering Journal, 158*, 173–180.

Almeida, C. A. P., Debacher, N. A., Downs, A. J., Cottet, L., & Mello, C. A. D. (2009). Removal of methylene blue from colored effluents by adsorption on montmorillonite clay. *Journal of Colloid Interface Science, 332*, 46–53.

Almeida, C. A. P., Santos, A., Jaerger, S., Debacher, N. A., & Hankins, N. P. (2010). Mineral waste from coal mining for removal of astrazon red dye from aqueous solutions. *Desalination, 264*, 181–187.

Altenor, S., Carene, B., Emmanuel, E., Lambert, J., & Gaspard, S. (2009). Adsorption studies of methylene blue and phenol onto vetiver roots activated carbon prepared by chemical activation. *Journal of Hazardous Materials, 165*, 1029–1039.

Antunes, M., Esteves, V. I., Guégan, R., Crespo, J. S., Fernandes, A. N., & Giovanela, M. (2012). Removal of diclofenac sodium from aqueous solution by Isabel grape bagasse. *Chemical Engineering Journal, 192*, 114–121.

Arasteh, R., Masoumi, M., Rashidi, A. M., Moradi, L., Samimi, V., & Mostafavi, S. T. (2010). Adsorption of 2-nitrophenol by multi-wall carbon nanotubes from aqueous solutions. *Applied Surface Science, 256*, 4447–4455.

Bhatnagar, A., Minocha, A. K., & Sillanpaa, M. (2010). Adsorptive removal of cobalt from aqueous solution by utilizing lemon peel as biosorbent. *Biochemical Engineering Journal, 48*, 181–186.

Brown, P. A., Gill, S. A., & Allen, S. J. (2000). Metal removal from wastewater using peat. *Water Research, 34*, 3907–3916.

Chang, Y., Lv, X., Zha, F., & Lei, Z. (2009). Sorption of p-nitrophenol by anion-cation modified palygorskite. *Journal of Hazardous Materials, 168*, 826–831.

Chowdhury, S., Chakraborty, S., & Saha, P. (2011). Biosorption of basic green 4 from aqueous solution by Ananas comosus (pineapple) leaf powder. *Colloids and Surface B, 84*, 520–527.

Cottet, L., Almeida, C. A. P., Naidek, N., Viante, M. F., Lopes, M. C., & Debacher, N. A. (2014). Adsorption characteristics of montmorillonite clay modified with iron oxide with respect to methylene blue in aqueous media. *Applied Clay Science, 95*, 25–31.

Couillard, D. (1994). The use of peat in wastewater treatment. *Water Research, 28*, 1261–1274.

Ding, L., Zou, B., Gao, W., Liu, Q., Wang, Z., Guo, Y., Wang, X., & Liu, Y. (2014). Adsorption of Rhodamine-B from aqueous solution using treated rice husk-based activated carbon. *Colloids and Surfaces A, 446*, 1–7.

Erdem, M., Yüksel, E., Tay, T., Çimen, Y., & Türk, H. (2009). Synthesis of novel methacrylate based adsorbents and their sorptive properties towards p-nitrophenol from aqueous solutions. *Journal of Colloid and Interface Science, 333*, 40–48.

Fernandes, A. N., Almeida, C. A. P., Menezes, C. T. B., Debacher, N. A., & Sierra, M. M. D. (2007). Removal of methylene blue from aqueous solution by peat. *Journal of Hazardous Materials, 144*, 412–419.

Fernandes, A. N., Almeida, C. A. P., Debacher, N. A., & Sierra, M. M. D. (2010a). Isotherm and thermodynamic data of adsorption of methylene blue from aqueous solution onto peat. *Journal of Molecular Structure, 982*, 62–65.

Fernandes, A. N., Giovanela, M., Esteves, V. I., & Sierra, M. M. D. (2010b). Elemental and spectral properties of peat and soil samples and their respective humic substances. *Journal of Molecular Structure, 971*, 33–38.

Fernandes, A. N., Giovanela, M., Almeida, C. A. P., Esteves, V. I., Sierra, M. M. D., & Grassi, M. T. (2011). Remoção dos hormônios 17β-estradiol e 17α-etinilestradiol de soluções aquosas empregando turfa decomposta como material adsorvente. *Quimica Nova, 34*, 1526–1533.

Freundlich, H. M. F. (1906). Uber die adsorption in losungen. *Zeitschrift für Physikalische Chemie, 57*, 385–470.

Girardello, F., Guégan, R., Esteves, V. I., Baumvol, I. J. R., Sierra, M. M. D., Crespo, J. S., Fernandes, A. N., & Giovanela, M. (2013). Characterization of Brazilian peat samples by applying a multimethod approach. *Spectroscopy Letters, 46*, 201–210.

Goulart, E.P. (1995). Matérias primas: Caracterização mineralógica, Curso Internacional de Treinamento em Grupo em Tecnologia Cerâmica, IPT/JICA, Cap. 5b.

Ho, Y. S. (2004). Citation review of Lagergren kinetic rate equation on adsorption reaction. *Scientometrics, 59*, 171–177.

Hu, Z., Chen, H., Ji, F., & Yuan, S. (2010). Removal of Congo Red from aqueous solution by cattail root. *Journal of Hazardous Materials, 173*, 292–297.

Huang, J., Yan, C., & Huang, K. (2008). Removal of p-nitrophenol by water-compatible hypercrosslinked resin functionalized with formaldehyde carbonyl groups and Xad-4 in aqueous solution: a comparative study. *Journal of Colloid Interface Science, 332*, 60–64.

Iram, M., Guo, C., Guan, Y., Ishfaq, A., & Liu, H. (2010). Adsorption and magnetic removal of neutral red dye from

aqueous solution using Fe$_3$O$_4$ hollow nanospheres. *Journal of Hazardous Materials, 181*, 1039–1050.

Jing, Q., Yi, Z., Lin, D., Zhu, L., & Yang, K. (2013). Enhanced sorption of naphthalene and p-nitrophenol by nano-SiO$_2$ modified with a cationic surfactant. *Water Research, 47*, 4006–4012.

Khenifi, A., Zohra, B., Kahina, B., Houari, H., & Zoubir, D. (2009). Removal of 2,4-DCP from wastewater by CTAB/bentonite using one-step and two-step methods: a comparative study. *Chemical Engineering Journal, 146*, 345–354.

Ko, C. H., Fan, C., Chiang, P. N., Wang, M. K., & Lin, K. C. (2007). p-Nitrophenol, phenol and aniline sorption by organo-clays. *Journal of Hazardous Materials, 149*, 275–282.

Krasil'nikova, O. K., Kul'kova, T. A., & Larin, A. V. (2008). Thermodynamics of the adsorption of 4-nitrophenol from aqueous solutions at activated charcoal. *Protection of Metals, 44*, 343–347.

Langmuir, I. (1916). The constitution and fundamental properties of solids and liquids. *Journal of the American Chemical Society, 38*, 2221–2295.

Li, K., Zheng, Z., Feng, J., Zhang, J., Luo, X., Zhao, G., & Huang, X. (2009). Adsorption of p-nitroaniline from aqueous solutions onto activated carbon fiber prepared from cotton stalk. *Journal of Hazardous Materials, 166*, 1180–1185.

Liu, B., Yang, F., Zou, Y., & Peng, Y. (2014a). Adsorption of phenol and p-nitrophenol from aqueous solutions on metal–organic frameworks: effect of hydrogen bonding. *Journal of Chemical & Engineering Data, 59*, 1476–1482.

Liu, D., Hao, L., & Fang, K. (2014b). Adsorption of cationic copolymer nanospheres onto cotton fibers investigated by a facile nephelometry. *Colloids and Surfaces A, 452*, 82–88.

Ma, Y., Zhou, Q., Li, A., Shuang, C., Shi, Q., & Zhang, M. (2014). Preparation of a novel magnetic microporous adsorbent and its adsorption behavior of p-nitrophenol and chlorotetracycline. *Journal of Hazardous Materials, 266*, 84–93.

Marco-Brown, J. L., Areco, M. M., Sánchez, R. M. T., & Afonso, M. S. (2014). Adsorption of picloram herbicide on montmorillonite: kinetic and equilibrium studies. *Colloids and Surfaces A, 449*, 121–128.

Mehrizad, A., Zare, K., Aghaie, H., & Dastmalchi, S. (2012). Removal of 4-chloro-2-nitrophenol occurring in drug and pesticide waste by adsorption onto nano-titanium dioxide. *International Journal of Environmental Science and Technology, 9*, 355–360.

Motsa, M. M., Thwala, J. M., Msagati, T. A. M., & Mamba, B. B. (2012). Adsorption of 2,4,6-trichlorophenol and ortho-nitrophenol from aqueous media using surfactant-modified clinoptilolite-polypropylene hollow fiber composites. *Water, Air, and Soil Pollution, 223*, 1555–1569.

Ngah, W. S. W., & Fatinathan, S. (2006). Chitosan flakes and chitosan-GLA beads for adsorption of p-nitrophenol in aqueous solution. *Colloids and Surfaces A, 277*, 214–222.

Nouri, S., & Haghseresht, F. (2004). Adsorption of p-nitrophenol in untreated and treated activated carbon. *Adsorption, 10*, 79–86.

Nourmohammadian, F., Davoodzadeh, M., & Alizadeh, A. A. (2007). New cyclopentadiene derivatives as novel pH indicators. *Dyes and Pigments, 74*(741–743), 2007.

Ofomaja, A. E., & Unuabonah, E. I. (2013). Kinetics and time-dependent Langmuir modeling of 4-nitrophenol adsorption onto Mansonia sawdust. *Journal of the Taiwan Institute of Chemical Engineers, 44*, 566–576.

Oller, I., Malato, S., & Sánchez-Pérez, J. A. (2011). Combination of advanced oxidation processes and biological treatments for wastewater decontamination—a review. *Science of the Total Environment, 409*, 4141–4166.

Ozcan, A., Oncu, E. M., & Ozcan, A. S. (2006). Kinetics, isotherm and thermodynamic studies of adsorption of Acid Blue 193 from aqueous solutions onto natural sepiolite. *Colloids and Surfaces A, 277*, 90–97.

Pan, B., Chen, X., Pan, B., Zhang, W., Zhang, X., & Zhang, Q. (2006). Preparation of an aminated macroreticular resin adsorbent and its adsorption of p-nitrophenol from water. *Journal of Hazardous Materials, 137*, 1236–1240.

Petroni, S. L. G., Pires, M. A. F., & Munita, C. S. (2000). Adsorção de zinco e cádmio em colunas de turfa. *Quimica Nova, 23*, 477–481.

Ringqvist, L., Holmgren, A., & Öborn, I. (2002). Poorly humified peat as an adsorbent for metals in wastewater. *Water Research, 36*, 2394–3404.

Romero-Gonzalez, J., Peralta-Videa, J. R., Rodriguez, E., Ramirez, S. L., & Gardea-Torresdey, J. L. (2005). Determination of thermodynamic parameters of Cr(VI) adsorption from aqueous solution onto Agave lechuguilla biomass. *The Journal of Chemical Thermodynamics, 37*, 343–347.

Rovani, S., Fernandes, A. N., Prola, L. D. T., Lima, E. C., Santos, W. O., & Adebayo, M. A. (2014). Removal of cibacron brilliant yellow 3G-P dye from aqueous solutions by brazilian peats as biosorbents. *Chemical Engineering Communications, 201*, 1431–1458.

Saha, P., Chowdhury, S., Gupta, S., & Kumar, I. (2010). Insight into adsorption equilibrium, kinetics and thermodynamics of Malachite Green onto clayey soil of Indian origin. *Chemical Engineering Journal, 165*, 874–882.

Shao, Y., Zhang, H., & Yan, Y. (2013). Adsorption dynamics of p-nitrophenol in structured fixed bed with micro entrapped activated carbon. *Chemical Engineering Journal, 225*, 481–488.

Tang, D., Zheng, Z., Lin, K., Luan, J., & Zhang, J. (2007). Adsorption of p-nitrophenol from aqueous solutions onto activated carbon fiber. *Journal of Hazardous Materials, 143*, 49–56.

Tewari, B. B. (2014). Removal of p-aminophenol and nitrophenol from aqueous solution through adsorption on bismuth, lead, and manganese ferrocyanides and their relevance to environmental issues. *Russian Journal of Physical Chemistry, 88*, 1564–1568.

Twardowska, I., Kysiol, J., Goldrath, T., & Avnimelech, Y. (1999). Adsorption of zinc onto peat from peatlands of Poland and Israel. *Journal of Geochemical Exploration, 66*, 387–405.

Weber, W. J., Jr., & Morris, J. C. (1963). Kinetics of adsorption on carbon from solution. *Journal of the Sanitary Engineering Division, 89*, 31–60.

Xue, G., Gao, M., Gu, Z., Luo, Z., & Hu, Z. (2013). The removal of p-nitrophenol from aqueous solutions by adsorption using gemini surfactants modified montmorillonites. *Chemical Engineering Journal, 218*, 223–231.

Yao, Y., Xu, F., Chen, M., Xu, Z., & Zhu, Z. (2010). Adsorption behavior of methylene blue on carbon nanotubes. *Bioresource Technology, 101*, 3040–3046.

Yao, Y.-X., Li, H.-B., Liu, J.-Y., Tan, X.-L., Yu, J.-G. & Peng, Z.-G. (2014). Removal and adsorption of p-nitrophenol from aqueous solutions using carbon nanotubes and their composites. *Journal of Nanomaterials*, 1–9.

Ye, P., & Lemley, A. T. (2009). Adsorption effect on the degradation of 4,6-o-dinitrocresol and p-nitrophenol in a montmorillonite clay slurry by AFT. *Water Research, 43*, 1303–1312.

Yuan, X., Sun, H., & Guo, D. (2012). The removal of COD from coking wastewater using extraction replacement-biodegradation coupling. *Desalination, 289*, 45–50.

Zhi-rong, L., Li-min, Z., Peng, W., Kai, Z., Chuan-xi, W., & Hui-hua, L. (2008). Competitive adsorption of heavy metal ions on peat. *Journal of China University of Mining and Technology, 18*, 255–260.